

Toughening mechanism of Hybrid Fiber Reinforced Cement Composites

H. Mihashi & Y. Kohno

Tohoku University, Sendai, Japan

ABSTRACT: A new type of fiber reinforced cement composites (FRCC) has been developed by means of hybrid fiber reinforcement in which randomly distributed short fibers of two types rationally bridge crack surfaces. They are steel cord and polyethylene fibers. In this paper, toughening mechanisms of this newly developed cement composite material are experimentally studied. Focused on the bridging mechanism of steel cord on the crack surface, pull-out tests on a single fiber embedded in cement-based matrixes are carried out to clarify the toughening mechanisms taking into account influences of the inclination angle, surface property and length of the fiber, including mechanical property of the matrix.

1 INTRODUCTION

Concrete is widely used in the world as the most common and important construction material. Although it is good at resisting under compression, plain concrete is a brittle material and the strength and strain capacity under tension are much lower than that under compression. From ancient times, it was well-known that poor crack resistance of brittle materials such as brick under tension is improved by fiber reinforcement. In the field of concrete engineering, extensive research works have been carried out on developing FRCC technology since the early 1960s and a wide range of practical applications was developed. Especially in these two decades, new types of fibers and material design methodologies have been developed. Processes of the development are reviewed in several books such as Bentur & Mindess (1990), Balaguru & Shah (1992) and Brandt (1995). Now several high performance fiber reinforced cement composites (HPFRCC) are available in practice. They can be found, for example, in the special issues of *Journal of Advanced Concrete Technology* (Japan Concrete Institute 2003 and 2006), an international journal published by Japan Concrete Institute.

Mechanical properties of brittle cement-based materials such as energy absorption and ductility can be significantly improved by reinforcing with fibers. Although fiber reinforcement generally doesn't improve the crack initiation strength, it does change the post-cracking behavior by bridging across the cracked surfaces. The crack bridging efficiency of a fiber depends on its length, interfacial properties,

geometry, diameter, mechanical properties such as Young's modulus and strength of the fiber as well as mechanical properties of the matrix.

Mechanisms of the crack bridging are usually studied with fiber pull-out tests. Since short fibers in FRCC are randomly distributed in the matrix, the orientation effect of fibers crossing the crack surface is also taken into consideration. There are many papers published on fiber pull-out tests. Pull-out tests on steel fibers with different profile and the inclination angle to the crack surface were carried out to study the influence of fiber geometry and the mix proportion of the matrix on the bond properties (e.g. Banthia et al. 1994, Naaman 1999).

Generally speaking, increasing the lateral surface of a fiber increases frictional and adhesive bond forces along the fiber to increase the pull-out resistance. However, deformed fiber such as screw may have a too strong grip to achieve a ductile behavior, though it may increase the pull-out strength. Naaman (1999) carried pull-out tests on smooth, hooked and twisted fibers and concluded that twisting is the best way to improve the mechanical component of bond of fibers.

Pull-out tests on inclined fibers were carried out by various researchers, too. Morton & Groves (1974) clearly showed that substantial stress concentration occurred in the matrix near the fiber exit point where the matrix always yields in compression. They also introduced a theoretical model based on elementary beam theory in which interfacial shear stress was neglected and the reaction stress from the matrix on the fiber was equal to the matrix yield strength. Brandt (1985) extended the analytical

model in which the fracture energy was given by summing the energy absorbed in the following five processes as a function of the inclination angle: 1) debonding of the fibers from the matrix; 2) pulling-out of fibers against the interfacial friction; 3) plastic deformation of the fibers; 4) yielding of the matrix in compression near the exit points of the fibers; 5) complementary friction between the fibers and the matrix due to local compression at the bending points.

Naaman & Shah (1976) carried out an experimental study on pull-out mechanism in steel fiber-reinforced concrete and concluded that spalling and disruption of the mortar matrix lead to a substantial reduction in the pull-out resistance. They also reported that as the number of fibers increases, the contribution of randomly oriented fibers relative to that of parallel fibers decreases. On the basis of a set of experiments with synthetic fibers, Li et al. (1990) reported that the increase of pull-out resistance is due to the additional friction stress caused by snubbing effect. Leung et al. (1992, 1995) developed a model to analyze the fiber bending/matrix spalling mechanisms by a micro mechanical approach, in which beam was bent on an elastic foundation with variable stiffness and with possibility of spalling. The theoretical analyses showed that the presence of an optimal yield strength for inclined fiber is due to the increased matrix spalling with increasing fiber yield strength. It was proved by an experimental work (Leung & Shapiro 1999).

In spite of the large number of studies, only a limited number of FRCC have achieved the high performance that accompanies a pseudo strain-hardening property and multiple cracking (Reinhardt and Naaman 1995). For example, Li & Leung (1992) developed Engineered Cementitious Composite (ECC) with synthetic fibers on the basis of a micro mechanical approach, in which the volume content of the synthetic fiber is less than 2%. In their work, it was clarified that bridging and snubbing friction of fibers on cracked surfaces under a certain condition are the key to achieve the multiple cracking which increases the ductility. On the other hand, Naaman (1999) developed a new type of deformed fiber by twisting triangular or rectangular steel fibers, which can achieve the high performance with a fiber volume content of less than 2% (Naaman 2003).

Besides changing the type and properties of the fiber, other various attempts have been made to develop new and improved FRCC systems, too. One of such attempts is hybrid fiber reinforcement systems. The combination of different types of fibers has been studied. For example, Rossi et al. (1987) presented an idea that fibers play a role at two different levels: at the material level, fibers can improve the strength and the ductility of concrete if a high per-

centage of fibers with a small diameter is used; at the structural level, fibers can improve the load bearing capacity and the ductility of the structure by using a low percentage of fibers long enough to allow sufficient anchorage. In the multi-scale concept (Rossi 1997, 2000), it is conceptually supposed that a large number of short and thinner metal fibers can "sow up" microcracks during the first stage of loading and then lower percentages of long metal fibers can also "sow up" the macrocracks during the stage of macrocrack propagation. Lawler et al. (2005) also suggested that microfibers delay the formation of macrocracks to increase the strength and toughness of the composites. However, there are quite few studies on the toughening mechanisms in the hybrid FRCCs.

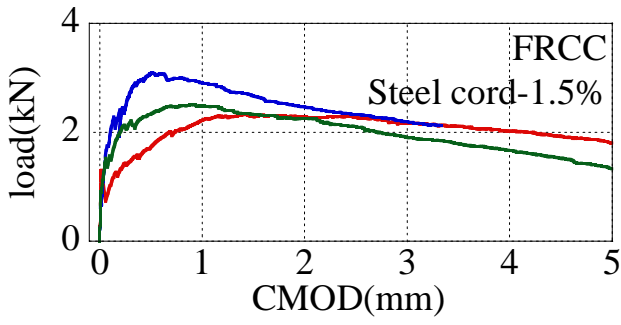
Kawamata et al. (2000, 2003) developed a new hybrid FRCC using steel cord and polyethylene fibers. Bending tests on notched beams clearly showed that the hybrid fiber reinforcement substantially improved the ductility, though the peak load was almost same as that of the virtual composite (Fig. 1). Cracking patterns observed in FRCC specimens containing only steel cord were very different from those in specimens reinforced with both of steel cord and polyethylene fibers together (Fig. 2). A parametric study was also carried out about the influence of materials and mixproportions on the mechanical properties. Length and volume content of the steel cord and water-cement ratio of the matrix were the dominant influencing factors. Uniaxial tension tests on cylindrical specimens made with an optimized mixproportion of this type of hybrid FRCC showed the pseudo strain-hardening until the strain of about 1.5% and multiple cracking.

The main objective of the present paper is to clarify the toughening mechanism of the hybrid FRCC using steel cord and polyethylene fibers. An experimental program of pull-out tests is carried and the toughening mechanism is discussed. Besides a single steel cord embedded in hardened cement paste (hcp) reinforced with short polyethylene fiber, a single straight steel fiber embedded in plain hcp as a reference as well as a single steel cord embedded in plain hcp are pulled out. The inclination angle of the fiber and the embedded length are varied, too.

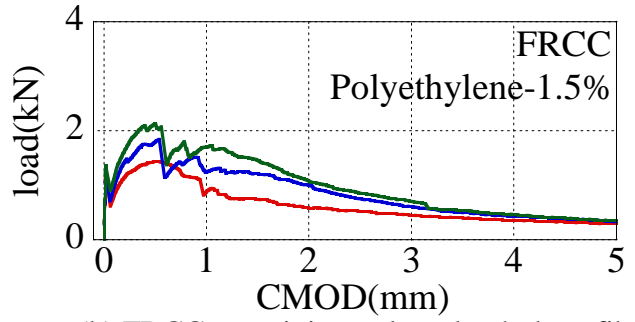
2 EXPERIMENTAL PROGRAM

2.1 Test groups

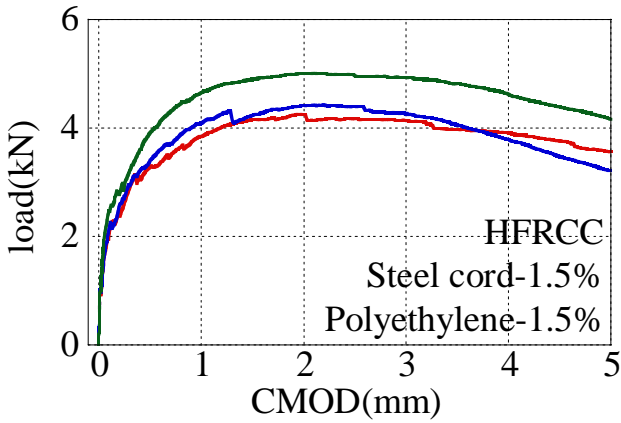
There were three groups of pull-out tests, each of which has the different combination of the pulled-out fiber and the matrix. Two types of steel fiber (steel cord: SC and straight fiber: SF) and two types of matrix (plain hardened cement paste: PLM and hardened cement paste reinforced with polyethylene fiber: PEM) were employed. In all series, the



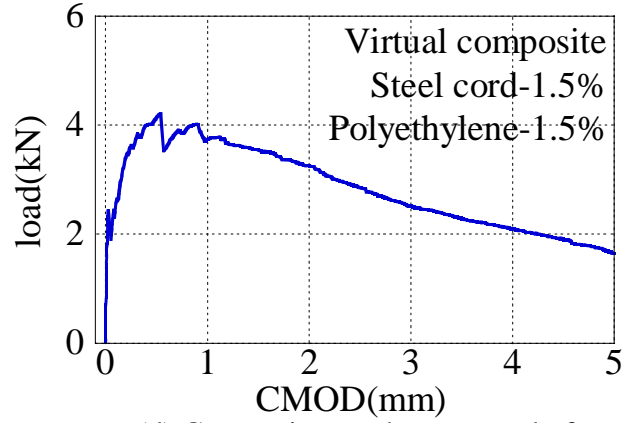
(a) FRCC containing only steel cord.



(b) FRCC containing only polyethylene fiber.

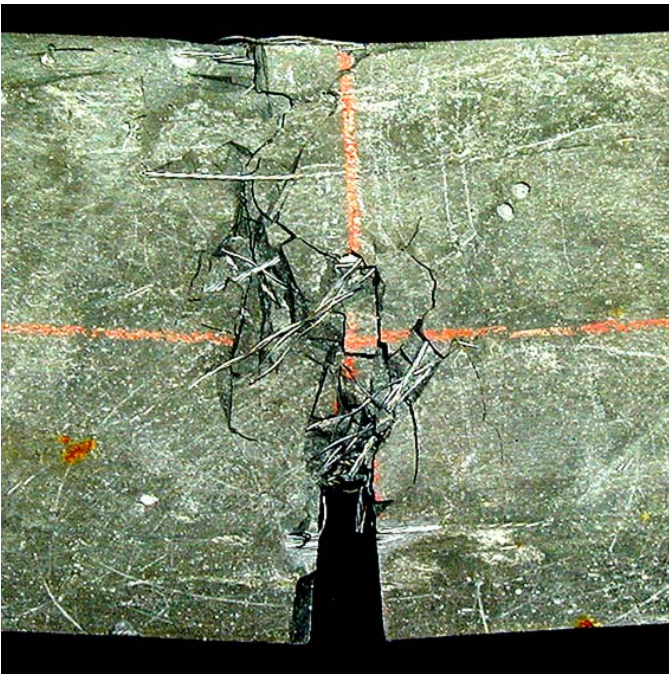


(c) HFRCC containing both steel cord and polyethylene fiber.

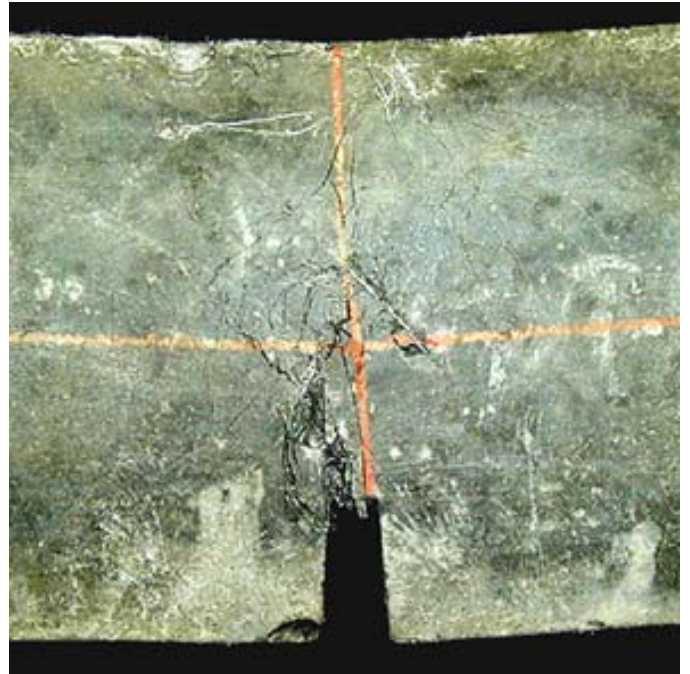


(d) Composite graph composed of (a) and (b).

Figure 1. Load-CMOD curves of bending tests (Kawamata et al. 2003).



(a) FRCC containing only steel cord.



(b) HFRCC containing both steel cord and polyethylene fiber.

Figure 2. Cracking near notch of specimens (Kawamata et al. 2003).

influence of the angle of fiber orientation on the pull-out behavior was investigated and the inclination angle was changed to be 0°, 15°, 30°, 45° and 60°. Three specimens were tested for each test condition.

The first group was aimed at assessing the influence of the geometry of steel fiber embedded in PLM: one is the straight fiber and the other is the steel cord. All fibers were used without any treatment on the surface.

The second group of pull-out tests was conducted to assess the influence of the toughness of the matrix. Two different types of material for the matrix were used for this comparison. While PLM was very brittle, PEM was much more ductile than PLM.

The third group of experiments was aimed at assessing the influence of the embedded length of the fiber. A steel cord of four different length was embedded in PEM.

2.2 Materials

Properties of two types of steel fibers are shown in Table 1. Since the tensile strength of both steel fibers was high enough, the fiber was not broken during the pull-out tests. SC is composed of five thin

Table 1. Properties of steel fiber.

| | Length | Diameter | Tensile strength | Young's modulus |
|---------------------|--------|----------|------------------|-----------------|
| | mm | μm | MPa | GPa |
| Steel cord (SC) | 32.0 | 405 | 2,850 | 206 |
| Straight fiber (SF) | 32.5 | 401 | 2,335 | 210 |

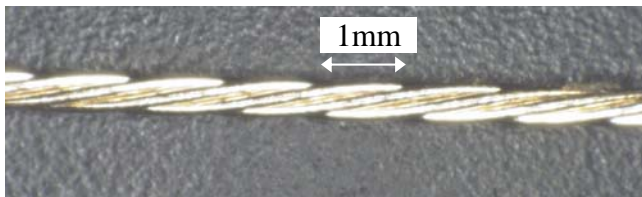


Figure 3. Profile of steel cord.

Table 2. Mix proportion of matrix.

| | W/B | SFM/B | SP/B | PE |
|--|------|-------|------|------|
| | wt% | wt% | wt% | vol% |
| Plain hardened cement paste (PLM) | 0.45 | 0.15 | 2 | 0 |
| Hardened cement paste reinforced with polyethylene (PEM) | 0.45 | 0.15 | 2 | 1 |

W: Water, C: High early strength Portland cement, SFM: Silica fume, B= C+SFM, SP: Superplasticizer, PE: Polyethylene fiber.

steel fibers whose diameter is about 135μm, and five of them are twisted together (see Fig. 3). On the other hand, SF had a smooth surface.

The mix proportions of the matrix are shown in Table 2. The material properties of the polyethylene fiber used in PEM matrix are as follows: length = 6mm, diameter = 12μm, Young's modulus = 75 GPa, tensile strength = 2,580MPa.

2.3 Specimen preparation

Fiber pull-out specimens with a steel fiber inclined at 0°, 15°, 30°, 45° and 60° were prepared with each type of fiber in Table 1 and matrix in Table 2, that is PLM-SF, PLM-SC and PEM-SC. Generally the embedded length was 16mm. In case of PEM-SC, however, the embedded length of the fiber was changed for four levels such as 16mm, 12mm, 8m, and 4mm. They are described as PEM-SC16, PEM-SC12, PEM-SC08 and PEM-SC04, respectively. The size of the pull-out specimen was 40mm × 35mm × 20mm. Before setting the mold, the fiber was first inserted into a small metal grip with a hole drilled at the appropriate angle in the middle (Fig. 4). A thin plastic sheet was glued with silicon grease

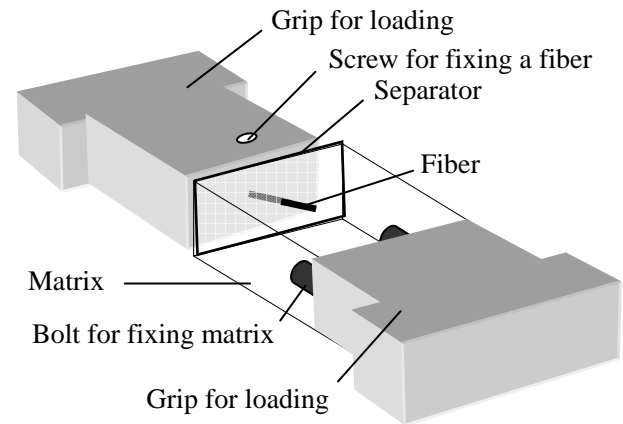


Figure 4. Metal grip for pull-out loading.

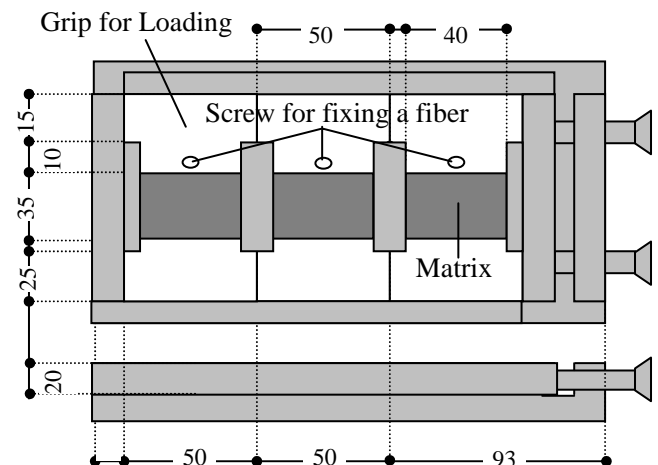


Figure 5. Mold for specimen preparation (unit: mm).

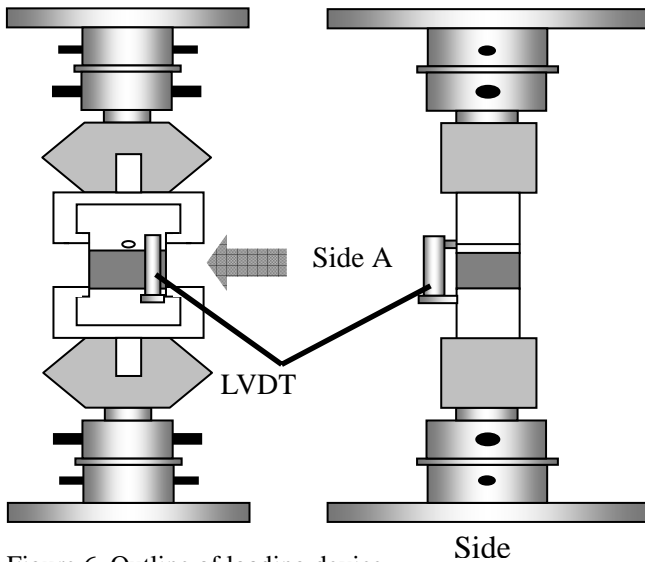


Figure 6. Outline of loading device.

to be a separator between the metal grip and the matrix, which works as the artificial crack surface. The embedded length of the fiber was left outside of the grip. After fixing the fiber in the grip with a screw, the grips were placed in a mold with three compartments (Fig. 5). Matrix was mixed with a bowl-mixer whose capacity was one liter. After casting and curing the specimens in a moisture room of 20°C and about 95%RH for seven days, they were loaded.

2.4 Pull-out testing

Outline of the loading device for the pull-out test is shown in Figure 6. After the specimen was carefully placed in the apparatus, a LVDT was placed between the grips for measuring the pull-out displacement. Loading was conducted by the displacement control with the rate of 0.2mm/sec.

3 EXPERIMENTAL RESULTS

While cylindrical specimens of $50\phi \times 100\text{mm}$ were tested, mean values of the compressive strength and the Young's modulus of the matrix were 42.4MPa and 24.7GPa for PLM, and 54.6MPa and 27.5GPa for PEM, respectively.

Figures 7-9 show the pull-out curves obtained for each experimental series. In PLM-SF series (Fig. 7), the adhesive bond strength was negligible as obviously shown in the case of zero inclination angle (0°, i.e. the fiber is embedded perpendicular to the crack surface) probably because of oil on the surface. Except in the case of 0°, there was a very steady ascending part between 15% and 60% of the embedded length and the peak load was obtained only after a large slip representing around 70% of the embedded length. The load level and the slope

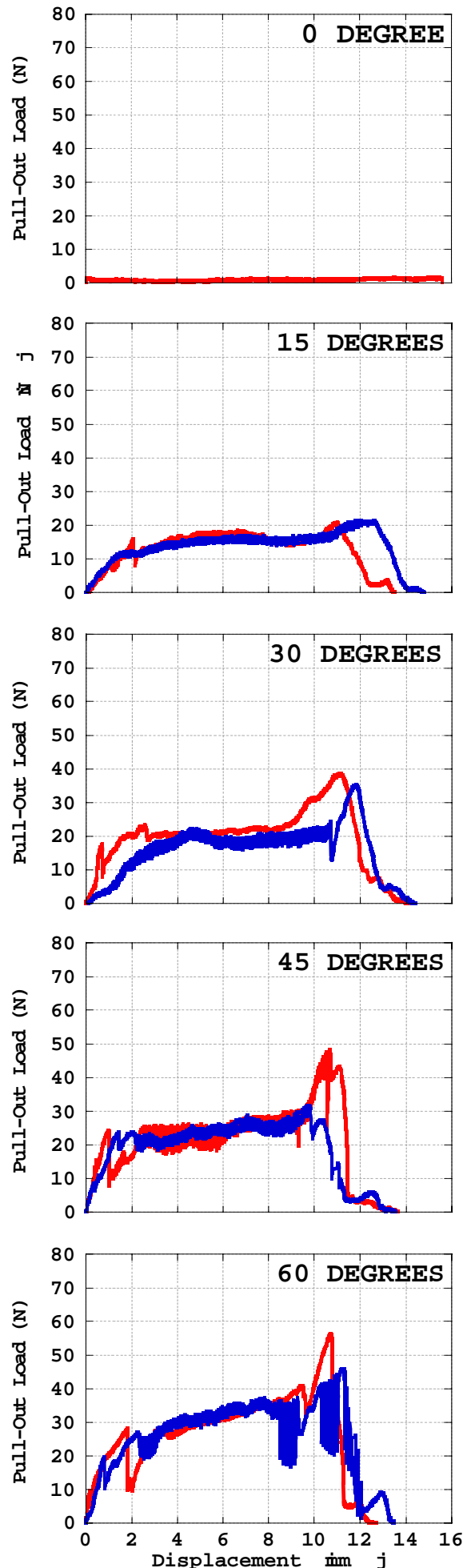


Figure. 7 Pull-out load vs. displacement curve (PLM-SF series).

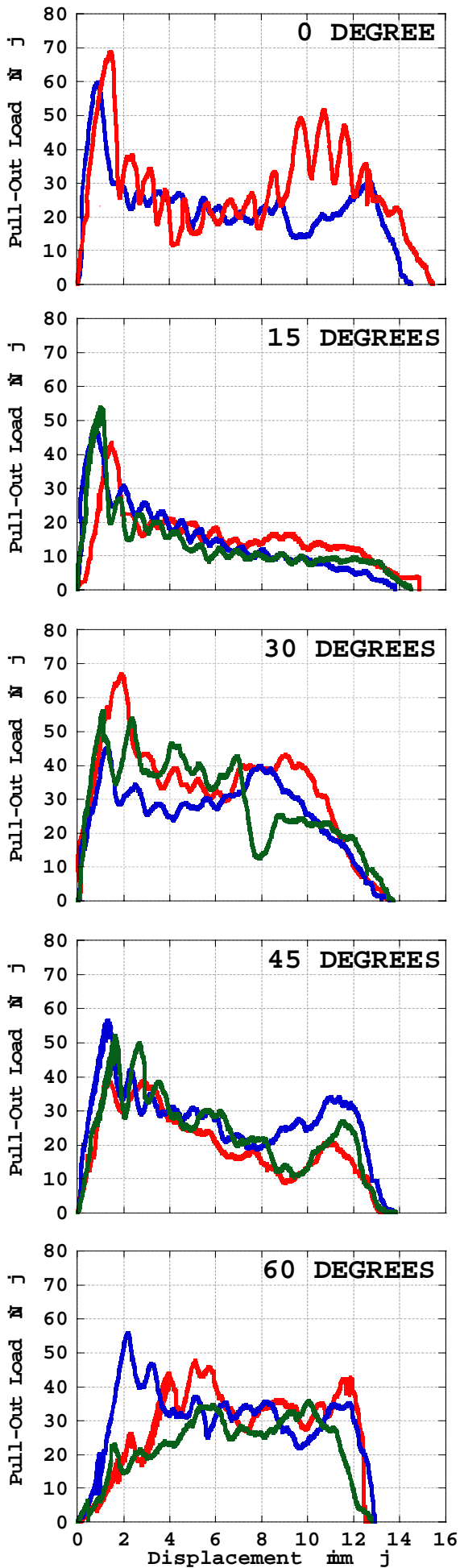


Figure 8. Pull-out load vs. displacement curve (PLM-SC series).

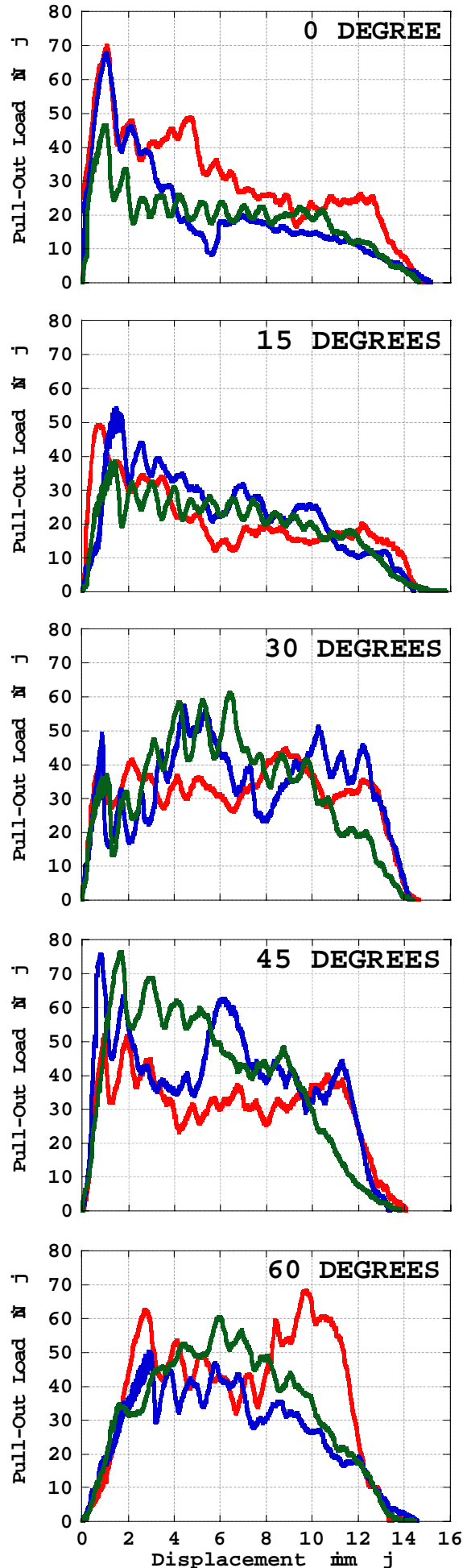


Figure 9. Pull-out load vs. displacement curve (PEM-SC16 series).

were almost proportional to the inclination angle. It might be caused by the frictional bond due to the compression stress at the fiber exit point since a fine stick-slip behavior of high frequency is observed on the curve.

Figure 8 shows the pull-out behavior of PLM-SC series. Even in the case of 0° , the peak load was very high and it was obtained in the early part of the pull-out curve. It means the peak load in this case is corresponding to the adhesive bond strength and the first peak represents the end of debonding along the fiber. Pull-out process after the debonding was composed of many small peaks whose cycle was about 1mm that is corresponding to the pitch (Fig. 3). Although the pull-out curve in the case of 15° descended monotonically after the peak, generally a high level of resistance was held. It is rather curious to find that some secondary peaks were observed around 60 to 70% of the embedded length in the case of 0° . It may mean that some untwisting of the steel cord occurs to increase the friction of the fiber. Although the load level was lower than that of the first peak, the last peak was observed around 75% of the embedded length in several curves. This tendency is similar to that in PLM-SF series.

Pull-out load versus displacement curves of PEM-SC series are shown in Figure 9, which shows a very high strength and ductility. As same as the curves in PLM-SC series, many small peaks were observed after the first peak. Especially over 30° of the inclination angle, the load levels were maintained at very high values which are almost equivalent to those of the first peaks.

Figure 10 shows the mean curves of PEM-SC series with the different embedded length of SC. As the inclination angle increases, the influence of the fiber length becomes significant.

4 DISCUSSION

4.1 Pull-out load and displacement curve

Figure 11 shows each mean curve of the relation between pull-out load and displacement in the three series. It is very obvious that the shape of the curve in case of PLM-SF is different from those in cases of PLM-SC and PEM-SC. Since the difference between two series of PLM-SF and PLM-SC is only properties of the steel fiber, the contributions of SC to the bridging can be found from the comparison. Significant characteristics of PLM-SC series are the high stiffness of the first ascending curve, the high load level of the first peak, and the periodic behavior after the first peak. These characteristics are observed in PEM-SC series, too. The slope of the first ascending part is very different between SF series and SC series. While the slope of SF series becomes higher as the inclination angle increases,

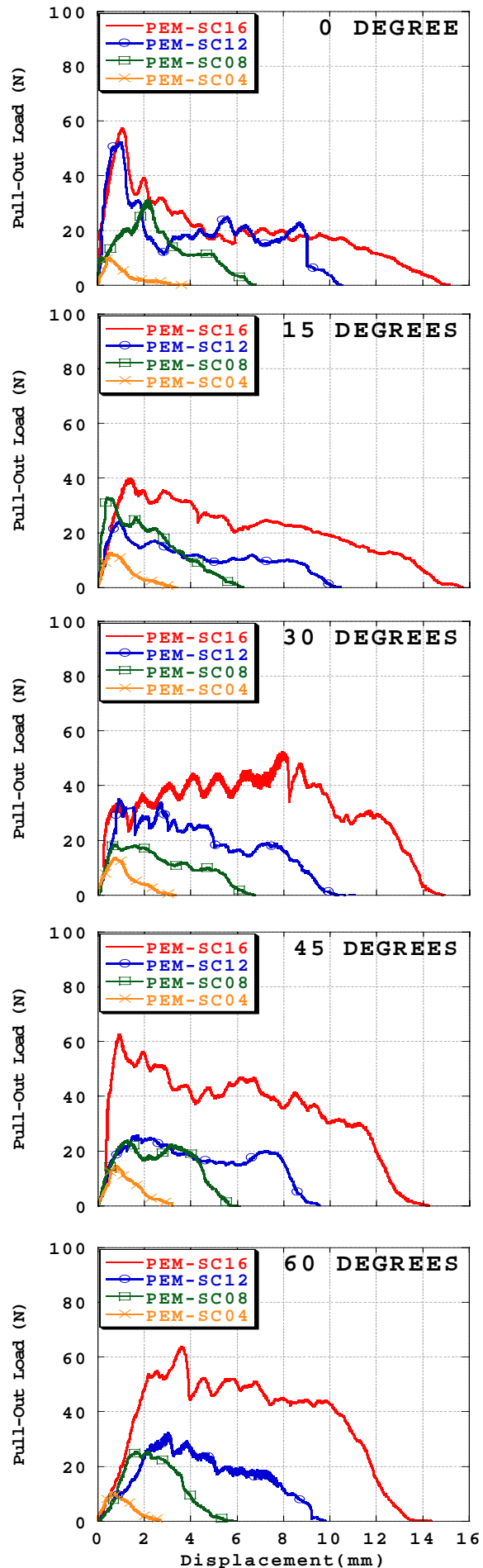


Figure 10. Mean curves of the relation between load and displacement (influence of embedded length in PEM-SC series).

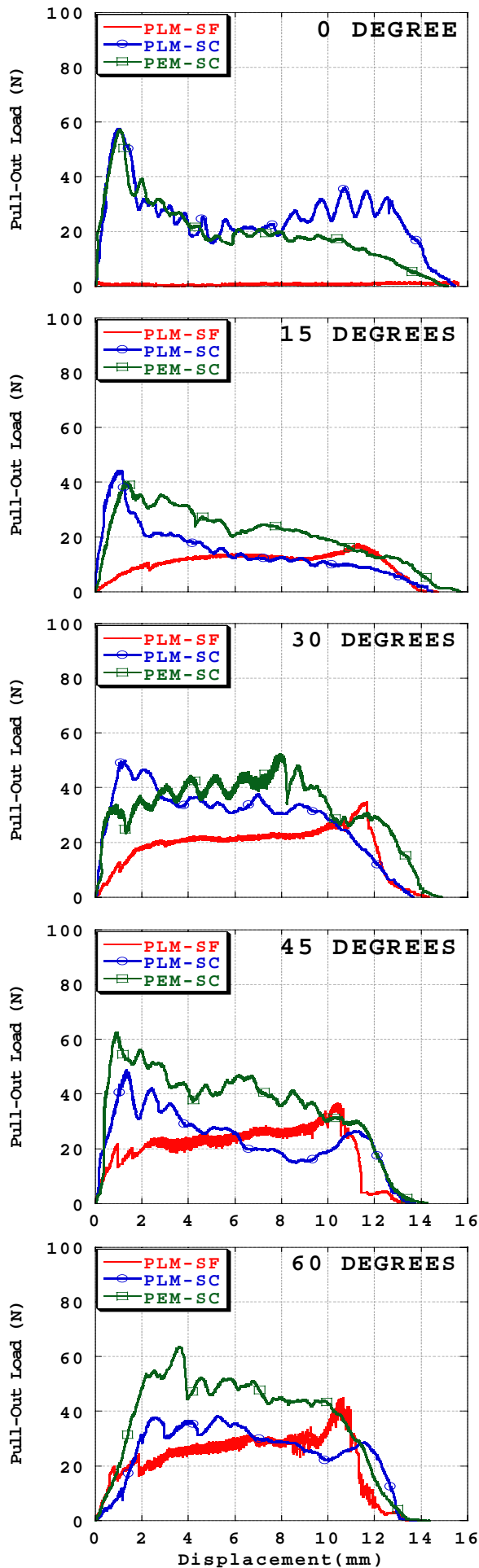


Figure 11. Mean curves of the relation between pull-out load and displacement in three series.

the changing process of SC series is not so obvious up to 30° . However, the slope remarkably decreases from 60° . These different tendencies may be related to the difference in the bridging mechanisms. The main mechanism of SF series is bending of the fiber and the frictional bond at the fiber exit point due to the compressive stress which increases as the inclination angle increases. On the other hand, the fiber of the SC series can resist directly to the pull-out load due to the high adhesive bond strength in the early stage of loading. As the inclination angle increases, the bending component of the stress for the local matrix at the fiber exit point becomes dominant and it causes a local failure of the matrix. It may be the reason why the slope in SC series suddenly decreases when the inclination angle becomes larger.

In PLM-SF series, the peak load was obtained just before the final pull-out. It may be because the fiber rotated as a short rigid cylinder and cut into the matrix (Leung & Shapio 1999). The post peak descending behavior of PLM-SF series is much steeper than that in other series. In several curves in case of PLM-SC series, the last peak similar to that in PLM-SF series was also observed around the displacement of 75% of the embedded length, though the load level was lower than that of the first peak. In PEM-SC16 series, however, the final peak was not observed as done in PLM-SF and PLM-SC series.

Since the crack width of multiple cracking observed in cylindrical specimen of hybrid FRCC was much less than 1mm (Kawamata et al. 2003), the most important parts in these curves are the first ascending part, the slope of this part, the first peak load and the post-peak behavior. From these view points, PEM-SC16 series achieves the highest performance especially for the cases of inclination angles higher than 45° . The peak loads and resistance levels after the first peak was obviously higher in case of PEM-SC16 series than those of PLM-SC series except in some limited number of portions.

4.2 Influence of the fiber length

In case of shorter embedded length (PEM-SC12, PEM-SC08, PEM-SC04 series), the peak loads and maintained resistance levels were mostly lower than those in PEM-SC16 series as shown in Figure 10. It was recognized that the influence of the fiber length is very significant from the view point of both strength and ductility. Now it is obvious that shorter steel cords can't sufficiently toughen the composite material even if the matrix is reinforced with synthetic fiber. These results are corresponding to the previous ones (Kawamata et al. 2003).

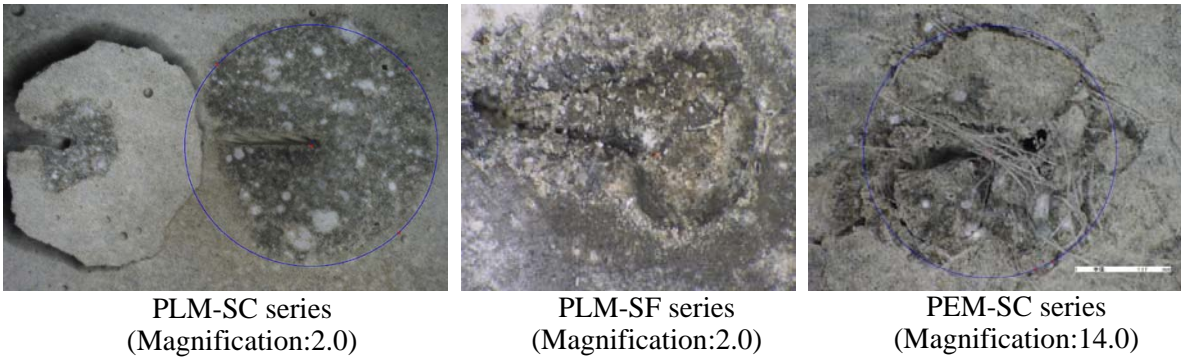


Figure 12. Matrix spalling from the fiber exit point (60 degree).

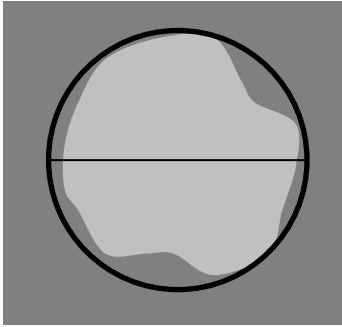


Figure 13. Measurement of diameter of matrix spalling.

4.3 Matrix spalling

As shown in previous studies, matrix failure at the fiber exit point is always observed in pull-out tests on inclined fibers. Typical examples observed in this study are shown in Figure 12. While cone type of the matrix failure was observed in cases of both PLM series, a much smaller portion damaged with many cracks was observed in case of PEM series. Since the difference of the test condition between PLM-SC series and PEM-SC16 series was only the matrix, the difference in the pull-out curves could be caused by the different cracking behavior around the fiber exit point.

Size of the matrix spalling was measured by the diameter of an envelope circle as shown in Figure 13. Relationship between the diameter and the inclined angle is significantly influenced by the type of matrix, fiber and the embedded length as shown in Figures 14-15. Because of the rough surface of SC, bond of the fiber might be too strong for hcp to prevent the cone failure in PLM-SC series. On the other hand, the higher crack resistance of the matrix at the fiber exit point prevents a large spalling of the matrix that is cone failure, though some microcracks were accumulated around the fiber (i.e. bond cracks) during the pull-out process. The small diameter in PEM-SC series may reflect the anchorage force of the fiber in the matrix on the pull-out resistance.

While Figure 14 shows the diameter is proportional to the inclination angle between 15°

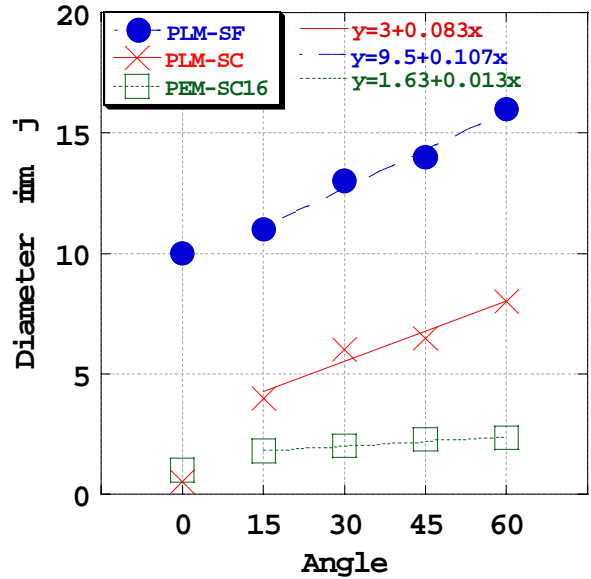


Figure 14. Diameter of matrix spalling and inclination angle (embedded length = 16mm).

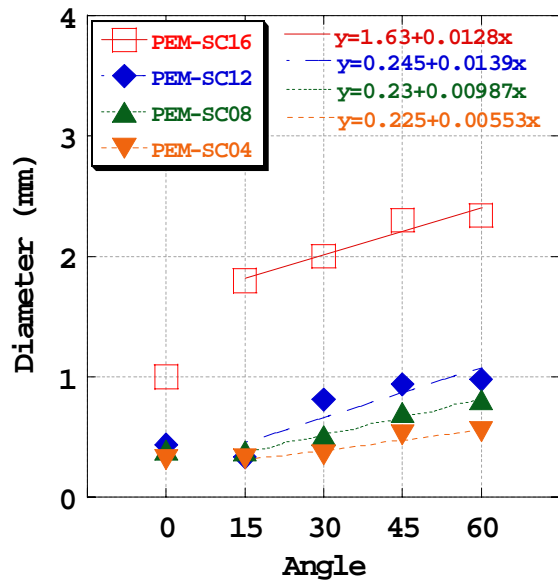


Figure 15. Diameter of matrix spalling and inclination angle (influence of embedded length).

and 60°, the diameter of PEM series is about 1/6 smaller than that of PLM series for the case of SC series. When the matrix is same, the diameter of PLM-SC series is always much larger than that of PLM-SF series. It is due to the very strong bond strength of the steel cord and it means that the critical condition to control the pull-out behavior of PLM-SC series is the cone creation in the matrix. However, even such a strong bond strength can't be sufficiently showed because of a limited space of the matrix if the fibers are densely distributed (Naaman & Shah 1976).

While Figure 15 shows the influence of the embedded length on the diameter of the matrix spalling is significant, the diameter is much smaller than that in case of PLM-SC series.

4.4 Absorbed energy

Absorbed energy during the pull-out test was calculated from the area under each load- displacement curve shown in Figures 7-9. Figure 16 shows the influence of the type of fiber and the matrix on the relation between the absorbed energy and the inclination angle. From this figure, it is obvious that the most dominant factor for the absorbed energy is the type of matrix on the condition with the sufficient fiber length. Especially when the inclination angle is over 30°, the absorbed energy in case of PEM-SC16 series is much higher than that in the corresponding case of PLM-SC series. It means that higher crack resistance of the matrix is the key to maintain the pull-out load up to the large displacement at least in the range of the inclination angle over 30°. If the size of the matrix spalling at the fiber exit point is small, the fiber can achieve a sufficient bridging up to a large displacement.

Figure 17 shows the absorbed energy remarkably decreases as the embedded length is shorter. Although the highest values were recorded in case of 30° for SC16 and SC12, the influence of the inclination angle on the absorbed energy was negligible for shorter fibers such as SC08 and SC04. Because of the shorter bridging length, friction due to the rough surface of the fiber can't work sufficiently for enhancing the load nor the energy absorption.

5 CONCLUSIONS

The obtained experimental results revealed that the high performance of the new hybrid FRCC is due to the high bond strength of the fiber with a sufficient length together with the high crack resistance of the matrix. Providing both factors is important because the former increases the pull-out strength and the latter improves the ductility.

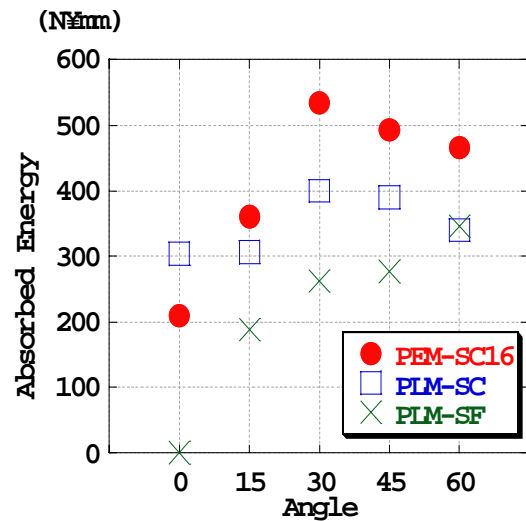


Figure 16. Relation between absorbed energy and inclination angle (embedded length = 16mm).

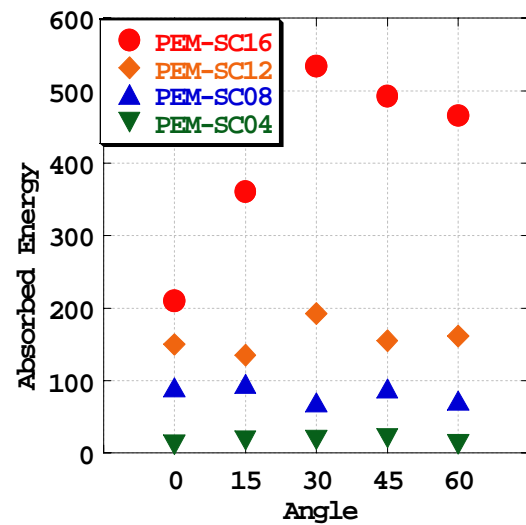


Figure 17. Relation between absorbed energy and inclination angle (influence of embedded length).

According to the experimental results and discussion presented in this paper, the following conclusions can be drawn:

- 1) Increased surface area of the steel cord leads to increasing adhesive and frictional bond forces along the fiber. It causes a significant increase in pull-out resistance which leads to a high strength.
- 2) Increased fracture energy of the matrix prevents a large spalling in the matrix at the fiber exit point. It maintains a high pull-out resistance and leads to high energy absorption and high ductility.
- 3) Appropriate material design of hybrid FRCCs is an efficient approach to develop further HPFRCCs.

ACKNOWLEDGEMENT

The partial financial support by Grant-in-Aid for Scientific Research of Japan Society for the Promotion of Science is gratefully acknowledged. The authors would like to express their thanks to

Tokyo Rope MFG. Co. for donating the steel fibers used in the investigation.

Rossi, P. Acker, P. and Mailer, P. 1987. Effect of Steel Fibers at Two Different Stages: *The Material and the Structure, Materials and Structures*, 20:436-439.

REFERENCES

- Banthia, N. Trottier, J.-F. & Pigeon, M. 1994. Concrete Reinforced with Deformed Steel Fibers, Part I: Bond-Slip Mechanisms, *ACI Material Journal*, 91(5): 435-446.
- Balaguru, P.N. & Shah, S.P. 1992. *Fiber Reinforced Cement Composites*. New York: McGraw-Hill, Inc.
- Bentur, A. & Mindess, S. 1990. *Fiber Reinforced Cementitious Composites*. London and New York: Elsevier Applied Science.
- Brandt, A.M. 1995. *Cement Based Composites*. London: E & FN Spon.
- Japan Concrete Institute 2003. Ductile Fiber Reinforced Cementitious Composites. *Journal of Advanced Concrete Technology*, 1(3): 211-340.
- Japan Concrete Institute 2006. *High-Performance Fiber Reinforced Cementitious Composites*, 4(1): 3-78.
- Kawamata, A. Mihashi, H. & Fukuyama, H. 2000. Flexural failure properties of hybrid fiber reinforced cementitious composites, *Proceedings of AIJ Tohoku Chapter Architectural Research Meeting*, (63): 69-72. (in Japanese)
- Kawamata, A., Mihashi, H. & Fukuyama, H. 2003. Properties of Hybrid Fiber Reinforced Cement-based Composites. *Journal of Advanced Concrete Technology*, 1(3): 283-290.
- Leung, C.K.Y. and Chi, J. 1995. Crack-Bridging Force in Random Ductile Fiber Brittle Matrix Composites. *Journal of Engineering Mechanics*, ASCE, 121(12): 1315-1324.
- Leung, C.K.Y. and Li, V.C. 1992. Effect of Fiber Inclination on Crack Bridging Stress in Brittle Fiber Reinforced Brittle Matrix Composites. *Journal of Mech. Phys. Solids*, 40(6): 1333-1362.
- Leung, C.K.Y. and Shapiro, N. 1999. Optimal Steel Fiber Strength for Reinforcement of Cementitious Materials. *Journal of Materials in Civil Engineering*, 11(2): 116-123.
- Leung, C.K.Y. and Ybanes, N. 1997. Pullout of Inclined Flexible Fiber in Cementitious Composite. *Journal of Engineering Mechanics*: 239-246
- Li, V.C., Wang, Y. and Backer, S. 1990. Effect of Inclining Angle, Bundling and Surface Treatment on Synthetic Fiber Pull-out from a Cement Matrix. *Composites*, 21(2): 132-140.
- Morton, J. and Groves, G.W. 1974. The Cracking of Composites Consisting of Discontinuous Ductile Fibers in a Brittle Matrix --- Effect of Fiber Orientation, *Journal of Material Science*, 9: 1436-1445.
- Naaman, A.E. 1999. Fibers with Slip-Hardening Bond. In Reinhardt H.W. and Naaman A.E. (eds.), *High Performance Fiber Reinforced Cement Composites (HPFRCC 3)*, Pro6, RILEM Publication S.A.R.L.: 371-385.
- Naaman, A.E. 2003. Engineered Steel Fibers with Optimal Properties for Reinforcement of Cement Composites, *Journal of Advanced Concrete Technology*, 1(3): 241-252.
- Naaman, A.E. and Reinhardt, H.W. (eds.). 1996. *High Performance Fiber Reinforced Cement Composites 2 (HPFRCC 2)*. London: E & FN Spon.
- Naaman, A.E. and Shah, S.P. 1976. Pull-out Mechanism in Steel Fiber-Reinforced Concrete. *Journal of the Structural Division*, ASCE, 102(8):1537-1548.
- Rossi, P. 1997. High Performance Multimodal Fiber Reinforced Composite (HPMFRCC): The LCPC experience. *ACI Material Journal*, 94(6): 478-483.
- Rossi, P. 2000. Ultra-High Performance Fiber Reinforced Concretes (HUPFRC): An overview. In Rossi, P. and Chanvilard, G. (eds.), *Fiber-Reinforced Concrete (FRC) – BEFIB 2000*, RILEM Publications S.A.R.L.: 87-100.